International Journal of Modern Engineering Research (IJMER)
www.ijmer.com Vol. 2, Issue. 5, Sep.-Oct. 2012 pp-3329-3339 ISSN: 2249-6645

Chemical reaction effect on an unsteady MHD free convection flow past an infinite vertical accelerated plate with constant heat flux, thermal diffusion and diffusion thermo

K. Sudhakar, R. Srinivasa Raju, and M. Rangamma

Department of Mathematics, University College of Science, Osmania University, Hyderabad, Andhra Pradesh, India.
Department of Mathematics, Padmasri Dr. B. V. Raju Institute of Technology, Narsapur, Medak, Andhra Pradesh, India.

Abstract: *The study of this paper to investigate the effect of chemical reaction on an unsteady magnetohydrodynamic free convection flow of a viscous incompressible fluid past an infinite vertical accelerated plate embedded in porous medium with thermal diffusion, diffusion thermo and constant heat flux in the presence of transverse magnetic field. The governing equations are solved by Galerkin finite element method. The results are obtained for velocity, temperature, concentration, skin friction, Nusselt number and Sherwood number. The effects of different flow parameters on the flow variables are discussed and presented through graphs and tables. And the numerical results for some special cases were compared with Chaudhary et al. [5] and were found to be in good agreement.*

Keywords: *Thermal diffusion, Diffusion thermo Unsteady, Free convection, MHD, Heat flux, Galerkin finite element method.*

Nomenclature:

C	Dimensionless concentration
ε	Porosity of the porous medium
C'_w	Concentration near the plate
C'_∞	Concentration in the fluid far
θ	Dimensionless Temperature away from the plate
T'	Temperature of the fluid
T'_w	Temperature of the plate
T'_∞	Temperature of the fluid far away from the plate
u'	Velocity component in x' – direction
x'	Spatial co – ordinate along the plate
ν	Kinematics viscosity, m^2/s plate
y'	Spatial co – ordinate normal to the plate
α	Thermal Diffusivity
k_e	Mean absorption coefficient
κ	Thermal conductivity, W/mK
σ	Electrical conductivity, mho/m
μ	Viscosity, Ns/m^2
μ_e	Magnetic permeability, Henry/meter
c_p	Specific heat at constant Pressure, J/kg-K
ρ	Density, kg/m^3
q'	Radiative heat flux
ω_e	Electron frequency, radian/sec
D	Chemical molecular diffusivity
τ_e	Electron collision time in Sec
U_o	Reference velocity
e	Electron charge, coulombs
M	Hartmann number
n_e	Number density of the electron
D_m	Mass diffusivity
k_T	Thermal diffusion ratio
c_s	Concentration susceptibility
T_m	Mean fluid temperature
$\Pr$	Prandtl number
P_e	Electron Pressure, N/ m^2
Sc	Schmidt Number
g	Acceleration due to Gravity, 9.81 m/s^2
Gr	Grashof Number
k_r	Chemical reaction parameter
β	Volumetric co–efficient of thermal Expansion, K^{-1}
Gc	Modified Grashof Number
Sr	Soret number
Du	Dufour number
β^*	Co – efficient of volume expansion with Species concentration

I. Introduction

The phenomenon of hydromagnetic flow with heat and mass transfer in an electrically conducting fluid past a porous plate embedded in a porous medium has attracted the attention of a good number of investigators because of its varied applications in many engineering problems such as MHD generators, plasma studies, nuclear reactors, oil exploration, geothermal energy extractions and in the boundary layer control in the field of aerodynamics. Heat transfer in laminar flow is important in problems dealing with chemical reactions and in dissociating fluids. Combined heat and mass transfer problems with chemical reaction are of importance in many processes and have, therefore, received a considerable amount of attention in recent years. In processes such as drying, evaporation at the surface of a water body, energy transfer in a wet cooling tower and the flow in a desert cooler, heat and mass transfer occur simultaneously. Possible applications of this type of flow can be found in many industries. For example, in the power industry, among the methods of generating electric power is one in which electrical energy is extracted directly from a moving conducting fluid. Many practical diffusive operations involve the molecular diffusion of a species in the presence of chemical reaction within or at the boundary. There are two types of reactions, homogeneous reaction and heterogeneous reaction. A homogeneous reaction is one that occurs uniformly throughout a given phase. The species generation in a homogeneous reaction is analogous to internal source of heat generation. In contrast, a heterogeneous reaction takes place in a restricted region or within the boundary of a phase. It can therefore be treated as a boundary condition similar to the constant heat flux condition in heat transfer.

The study of heat and mass transfer with chemical reaction is of great practical importance to engineers and scientists because of its almost universal occurrence in many branches of science and engineering. The flow of a fluid past a wedge is of fundamental importance since this type of flow constitutes a general and wide class of flows in which the free stream velocity is proportional to a power of the length coordinate measured from the stagnation point. All industrial chemical processes are designed to transform cheaper raw materials to high value products (usually via chemical reaction). A 'reactor', in which such chemical transformations take place, has to carry out several functions like bringing reactants into intimate contact, providing an appropriate environment (temperature and concentration fields) for adequate time and allowing for removal of products. Fluid dynamics plays a pivotal role in establishing relationship between reactor hardware and reactor performance. For a specific chemistry catalyst, the reactor performance is a complex function of the underlying transport processes. The first step in any reaction engineering analysis is formulating a mathematical framework to describe the rate (and mechanisms) by which one chemical species is converted into another in the absence of any transport limitations (chemical kinetics). Once the intrinsic kinetics is available, the production rate and composition of the products can be related, in principle, to reactor volume, reactor configuration and mode of operation by solving mass, momentum and energy balances over the reactor. This is the central task of a reaction and reactor engineering activity. Analysis of the transport processes and their interaction with chemical reactions can be quite difficult and is intimately connected to the underlying fluid dynamics. Such a combined analysis of chemical and physical processes constitutes the core of chemical reaction engineering. Recent advances in understanding the physics of flows and computational flow modeling (CFM) can make tremendous contributions in chemical engineering.

In view of its wide applications, Acharya *et al.* [1] have reported the problem of heat and mass transfer over an accelerating surface with heat source in presence of suction and blowing. Chamkha and Takhar [3] are used the blotter difference method to study laminar free convection flow of air past a semi infinite vertical plate in the presence of chemical species concentration and thermal radiation effects. Chandran and his associates [4] have discussed the unsteady free convection flow of an electrically conducting fluid with heat flux and accelerated boundary layer motion in presence of a transverse magnetic field. Chaudhary *et al.* [5] studied the effect of free convection effects on magnetohydrodynamic flow past an infinite vertical accelerated plate embedded in porous media with constant heat flux by using Laplace transform technique for finding the analytical solutions. Das and Mitra [6] discussed the unsteady mixed convective MHD flow and mass transfer past an accelerated infinite vertical plate with suction. Recently, Das and his co – workers [7] analyzed the effect of mass transfer on MHD flow and heat transfer past a vertical porous plate through a porous medium under oscillatory suction and heat source. Das *et al.* [8] investigated numerically the unsteady free convective MHD flow past an accelerated vertical plate with suction and heat flux. Das and his associates [9] estimated the mass transfer effects on unsteady flow past an accelerated vertical porous plate with suction employing finite difference analysis.

Gireesh kumar *et al.* [10] investigated effects of chemical reaction and mass transfer on MHD unsteady free convection flow past an infinite vertical plate with constant suction and heat sink. Hasimoto [11] initiated the boundary layer growth on a flat plate with suction or injection. Ibrahim [12] studied the effects of chemical reaction and radiation absorption on transient hydromagnetic natural convection flow with wall transpiration and heat source. Jha [13] analyzed the effect of applied magnetic field on transient free convective flow in a vertical channel. The unsteady free convective MHD flow with heat transfer past a semi-infinite vertical porous moving plate with variable suction has been studied by Kim [14]. Makindeet *et al.* [15] discussed the unsteady free convective flow with suction on an accelerating porous plate. Mansutti *et al.* [16] have discussed the steady flow of a non – Newtonian fluid past a porous plate with suction or injection. Sarangi and Jose [18] studied the unsteady free convective MHD flow and mass transfer past a vertical porous plate with variable temperature. Sharma and Pareek [19] explained the behaviour of steady free convective MHD flow past a vertical porous moving surface. Singh and his co – workers [20] have analyzed the effect of heat and mass transfer in MHD flow of a viscous fluid past a vertical plate under oscillatory suction velocity. Singh and Thakur [21] have given an exact solution of a plane unsteady MHD flow of a non – Newtonian fluid. Soundalgekar [22] showed the effect of free convection on steady MHD flow of an electrically conducting fluid past a vertical plate. Yamamoto and Iwamura [23] explained the flow of a viscous fluid with convective acceleration through a porous medium.

Motivate by above reference work, it is proposed here to study the effect of chemical reaction on an unsteady MHD free convection flow past an infinite vertical accelerated plate embedded in porous media with constant heat flux, thermal diffusion and diffusion thermo by Galerkin finite element method which is more economical from computational view point and The results obtained are good agreement with the results of Chaudhary *et al*. [5] in some special cases.

II. Mathematical analysis:

We consider a two – dimensional flow of an incompressible electrically conducting viscous fluid along an infinite non – conducting vertical flat plate through a porous medium. Initially, for time $t' \le 0,$ the plate and the fluid are at some temperature T'_∞ in a stationary condition with the same species concentration C'_∞ at all points. The x' – axis is taken along the plate in the vertically upward direction and the y' – axis is taken normal to the plate. At time $t' > 0$ a magnetic field of uniform strength is applied in the direction of y' – axis and the induced magnetic field is neglected. At time $t' > 0$, the plate starts moving impulsively in its own plane with a velocity U_o with heat supplied to the plate at constant rate. The governing equations of motion and energy under usual Boussinesq's approximation are given by:

Continuity Equation:

$$\frac{\partial v'}{\partial y'} = 0 \Rightarrow v' = -v'_o \text{ (Constant)} \tag{1}$$

Momentum Equation:

$$\frac{\partial u'}{\partial t'} = \nu \frac{\partial^2 u'}{\partial y'^2} - \frac{\sigma B_o^2 u'}{\rho} + g\beta(T' - T'_\infty) + g\beta^*(C' - C'_\infty) - \frac{\nu u'}{K'} \tag{2}$$

Energy Equation:

$$\frac{\partial T'}{\partial t'} = \frac{\kappa}{\rho c_p} \frac{\partial^2 T'}{\partial y'^2} + \frac{D_m k_T}{c_S c_p} \frac{\partial^2 C'}{\partial y'^2} \tag{3}$$

Diffusion Equation:

$$\frac{\partial C'}{\partial t'} = D \frac{\partial^2 C'}{\partial y'^2} - K'_r C' + \frac{D_m k_T}{T_m} \frac{\partial^2 T'}{\partial y'^2} \tag{4}$$

With the following initial and boundary conditions:

$$\left.\begin{array}{l} t' \le 0: \{u' = 0,\ T' = T'_\infty,\ C' = C'_\infty \quad for all\ y' \\ t' > 0: \left\{\begin{array}{l} u' = U_o,\ \dfrac{\partial T'}{\partial y'} = -\dfrac{q'}{\kappa'},\ C' = C'_w \ at\ y' = 0, \\ u' = 0,\ T' = T'_\infty,\ C' = C'_\infty\ at\ y' \to \infty \end{array}\right\} \end{array}\right\} \tag{5}$$

Introducing the following dimensionless quantities:

$$\left.\begin{array}{l} t = \dfrac{t'U_o^2}{\nu},\ y = \dfrac{U_o y'}{\nu},\ u = \dfrac{u'}{U_o},\ \Pr = \dfrac{\mu C_p}{\kappa}, Sc = \dfrac{\nu}{D},\ M = \dfrac{\sigma B_o^2 \nu}{\rho U_o^2}, Gr = \dfrac{\nu g\beta(T'_w - T'_\infty)}{U_o{}^3}, \\ Gc = \dfrac{g\beta^* \nu(C'_w - C'_\infty)}{U_o^3},\ K = \dfrac{U_o^2 K'}{\nu^2},\ \theta = \dfrac{T' - T'_\infty}{T'_w - T'_\infty},\ C = \dfrac{C' - C'_\infty}{C'_w - C'_\infty},.\ Du = \dfrac{D_m k_T (C'_w - C'_\infty)}{c_S c_P (T'_w - T'_\infty)}, \\ Sr = \dfrac{D_m k_T (T'_w - T'_\infty)}{\nu T_m (C'_w - C'_\infty)},\ k_r = \dfrac{K'_r \nu}{U_0^2} \end{array}\right\} \tag{6}$$

Using dimensionless quantities from (6), the equations (2), (3) and (4) reduces to

$$\frac{\partial^2 u}{\partial y^2} + (Gr)\theta + (Gc)C = \frac{\partial u}{\partial t} + (M + \frac{1}{K})u \tag{7}$$

$$\frac{\partial^2 \theta}{\partial y^2} = (\Pr)\frac{\partial \theta}{\partial t} - (\Pr)(Du)\left(\frac{\partial^2 C}{\partial y^2}\right) \tag{8}$$

$$\frac{\partial^2 C}{\partial y^2} = (Sc)\frac{\partial C}{\partial t} - (Sc)(Sr)\left(\frac{\partial^2 \theta}{\partial y^2}\right) + (Sc)(k_r)C \tag{9}$$

with the following initial and boundary conditions

$$\left.\begin{array}{l} t \le 0: \{u = 0,\ \theta = 0,\ C = 0 \ \ for\ all\ y \\ t > 0: \left\{\begin{array}{l} u = 1,\ \dfrac{d\theta}{dy} = -1,\ C = 1\ at\ y = 0 \\ u = 0,\ \theta = 0,\ C = 0\ at\ y \to \infty \end{array}\right\} \end{array}\right\} \tag{10}$$

All the physical variables are defined in the nomenclature.

III. Method of solution

Applying the Galerkin finite element method for equations (7) – (9) over the element (e) $(y_j \le y \le y_k)$ yields

$$\int_{y_j}^{y_k} N^{(e)^T} \left(\frac{\partial^2 \mathrm{u}^{(e)}}{\partial y^2} - \frac{\partial \mathrm{u}^{(e)}}{\partial t} - B\mathrm{u}^{(e)} + P \right) dy = 0 \tag{11}$$

$$\int_{y_j}^{y_k} N^{(e)^T} \left(\frac{\partial^2 \theta^{(e)}}{\partial y^2} - \Pr \frac{\partial \theta^{(e)}}{\partial t} + Q \right) dy = 0 \tag{12}$$

$$\int_{y_j}^{y_k} N^{(e)^T} \left(\frac{\partial^2 C^{(e)}}{\partial y^2} - Sc \frac{\partial C^{(e)}}{\partial t} - (Sc)(k_r)C^{(e)} + R \right) dy = 0 \tag{13}$$

Where $B = M + \dfrac{1}{k}$, $P = Gr\theta_i^j + GcC_i^j$, $Q = (\Pr)(Du)\left(\dfrac{\partial^2 C_i^j}{\partial y^2}\right)$, $R = (Sc)(Sr)\left(\dfrac{\partial^2 \theta_i^j}{\partial y^2}\right)$

Let the linear piecewise approximation solution be

$$u^{(e)} = N_j(y)u_j(t) + N_k(y)u_k(t) = N_j u_j + N_k u_k,$$

$$\theta^{(e)} = N_j(y)\theta_j(t) + N_k(y)\theta_k(t) = N_j \theta_j + N_k \theta_k,$$

$$C^{(e)} = N_j(y)C_j(t) + N_k(y)C_k(t) = N_j C_j + N_k C_k.$$

Where $N_j = \dfrac{y_k - y}{y_k - y_j}$, $N_k = \dfrac{y - y_j}{y_k - y_j}$, $N^{(e)T} = \begin{bmatrix} N_j & N_k \end{bmatrix}^T = \begin{bmatrix} N_j \\ N_k \end{bmatrix}$.

The differential equations (11) – (13) subjected to the boundary conditions (10) are highly non – linear and coupled, and cannot be solved analytically. Therefore, following Bathe [2] and Reddy [17], we use the finite element method to obtain an accurate and efficient solution to the boundary value problem under consideration. The fundamental steps comprising the method are as follows:

Step 1: Discretize the domain into elements:

The whole domain is divided into a finite number of sub – domains. Each sub – domain is termed by a finite element. The collection of the elements is designated to the finite element mesh.

Step 2: Derive the element equations:

The derivation of the finite element equations, i.e., the algebraic equations among the unknown parameters of the finite element approximation, involves constructing the variational formulation of the differential equation, assuming the form of the approximate solution over a typical finite element, and deriving the finite element equations by substituting the approximate solution into the variational formulation.

Step 3: Assemble the element equations:

The algebraic equations obtained are assembled by imposing the inter – element continuity conditions. This yields a large number of algebraic equations, which can constitute the global finite element model governing the whole flow domain.

Step 4: Impose the boundary conditions:

The physical boundary conditions defined in equation (10) are imposed on the assembled equations.

Step 5: Solve the assembled equations:

The final matrix equation can be solved by a direct or indirect (iterative) method. For computational purposes, the coordinate y varies from 0 to $y_{\max} = 10$, where $y_{\max}$ represents infinity, i.e., external to the momentum, energy, and concentration boundary layers. The whole domain is divided into 100 line elements with the equal width 0.05, and each element has three nodes. Therefore, after assembly of all the element equations, we obtain a matrix of the order 201 × 201. This obtained system of equations after assembly of the element equations is non – linear. Therefore, an iterative scheme is used to solve it. The system is linearized by incorporating the known functions. After applying the given boundary conditions only, a system of 195 equations remains for the solution which has been solved by using the Gauss elimination method. This process is repeated until the desired accuracy of 5×10^{-4} is obtained.

IV. Skin friction and rate of heat and mass transfer

The skin friction, Nusselt number and Sherwood number are important physical parameters for this type of boundary layer flow. The skin friction at the plate, which in the non – dimensional form is given by

$$\tau = \frac{\tau'_w}{\rho U_o v} = \left(\frac{\partial u}{\partial y}\right)_{y=0} \tag{14}$$

The rate of heat transfer coefficient, which in the non – dimensional form in terms of the Nusselt number is given by

$$Nu = -x\frac{\left(\frac{\partial T'}{\partial y'}\right)_{y'=0}}{T'_w - T'_\infty} \Rightarrow Nu\,\mathrm{Re}_x^{-1} = -\left(\frac{\partial \theta}{\partial y}\right)_{y=0} \tag{15}$$

The rate of mass transfer coefficient, which in the non – dimensional form in terms of the Sherwood number, is given by

$$Sh = -x\frac{\left(\frac{\partial C'}{\partial y'}\right)_{y'=0}}{C'_w - C'_\infty} \Rightarrow Sh\,\mathrm{Re}_x^{-1} = -\left(\frac{\partial C}{\partial y}\right)_{y=0} \tag{16}$$

Where $\mathrm{Re} = \frac{U_o x}{v}$ is the local Reynolds number.

V. Results and Discussions

In order to understand the effects of different parameters in the problem, velocity, temperature and concentration profiles, skin friction, Nusselt number and Sherwood number have been discussed by assigning numerical values to various parameters Grashof number (Gr), Modified Grashof number (Gc) Prandtl number (Pr), Schmidt number (Sc), Hartmann number (M), Permeability parameter (K), Soret number (Sr), Dufour number (Du) and Chemical reaction parameter (k_r) separately. We discussed the effects of material parameters on primary velocity profiles from figures (2) to (10), temperature profiles from figures (11) and (12) and concentration profiles from the figures (13) to (15). During the course of numerical calculations of the primary velocity (u), temperature (θ) and concentration (C) the values of the Prandtl number are chosen for Mercury (Pr = 0.025), Air at 25^oC and one atmospheric pressure (Pr = 0.71), Water (Pr = 7.00) and Water at 4^oC (Pr = 11.62). To focus out attention on numerical values of the results obtained in the study, the values of Sc are chosen for the gases representing diffusing chemical species of most common interest in air namely Hydrogen (Sc = 0.22), Helium (Sc = 0.30), Water – vapour (Sc = 0.60), Oxygen (Sc = 0.66) and Ammonia (Sc = 0.78). For the physical significance, the numerical discussions in the problem and at t = 1.0, stable values for primary velocity, secondary velocity, temperature and concentration fields are obtained. To examine the effect of parameters related to the problem on the velocity field and skin – friction numerical computations are carried out at Pr = 0.71. To find out the solution of this problem, we have placed an infinite vertical plate in a finite length in the flow. Hence, we solve the entire problem in a finite boundary. However, in the graphs, the y values vary from 0 to 4, and the velocity, temperature, and concentration tend to zero as y tends to 4. This is true for any value of y. Thus, we have considered finite length.

1.1 Velocity field

The velocity of the flow field is found to change more or less with the variation of the flow of nine parameters. The major factors affecting the velocity of the flow field are Grashof number (Gr), Modified Grashof number (Gc) Prandtl number (Pr), Schmidt number (Sc), Hartmann number (M), Permeability parameter (K), Soret number (Sr), Dufour number (Du) and Chemical reaction parameter (k_r). The effects of these parameters on the velocity field have been analyzed with the help of figures (2) to (10). Figure (2) shows the effect of Grashof number for heat transfer on velocity. The Grashof number Gr for heat transfer is found to enhance velocity at all points due to the action of free convection current in the flow field. Figure (3) presents the effect of Grashof number for mass transfer on velocity. The figure shows the accelerating effect of the parameter Gc on the velocity of the flow field at all points. In figure (4), we depict the effect of Prandtl number on velocity of the flow field. The presence of heavier Prandtl number in the flow field is found to decelerate velocity at all points. In figure (5) we depict the effect of Schmidt number on velocity of the flow field. The presence of heavier Schmidt number in the flow field is found to decelerate velocity at all points. The effect of Hartmann number M is shown in the figure (6). It is observed that the velocity of the fluid decreases with the increase of Hartmann number values. As expected, the velocity decreases with an increase in the Hartmann number. It is because that the application of transverse magnetic field will result in a resistive type force (Lorentz force) similar to drag force which tends to resist the fluid flow and thus reducing its velocity. Also, the boundary layer thickness decreases with an increase in the Hartmann number. We also see that velocity profiles decrease with the increase of magnetic effect indicating that magnetic field tends to retard the motion of the fluid. Magnetic field may control the flow characteristics. Figure (7) shows the effect of the permeability of the porous medium parameter (K) on the velocity distribution. As shown, the velocity is increasing with the increasing dimensionless porous medium parameter. The effect of the dimensionless porous medium K becomes smaller as K increase. Physically, this result can be achieved when the holes of the porous medium may be neglected. From figures (8) and (9), the effects of Soret and Dufour numbers on the velocity field are shown. We observe that the velocity increases with the increase of both Dufour and Soret number. Figure (10) displays the effect of the chemical reaction parameter (k_r) on the velocity profiles. As expected, the presence of the chemical reaction significantly affects the velocity profiles. It should be mentioned that the studied case is for a destructive chemical reaction (k_r). In fact, as chemical reaction (k_r) increases, the considerable reduction in the velocity profiles is predicted, and the presence of the peak indicates that the maximum value of the velocity occurs in the body of the fluid close to the surface but not at the surface.

5.2 Temperature field

The temperature of the flow field suffers a substantial change with the variation of the flow parameters such as Prandtl number $(\Pr)$ and Dufour number (Du) .These variations are shown in figures (11) and (12). An increase in Prandtl number decreases the Temperature field (figure (11)). Also, Temperature field falls more rapidly for Water in comparison to Air and the Temperature field curve is exactly linear for Mercury, which is more sensible towards change in Temperature. From this observation it is concluded that Mercury is most effective for maintaining Temperature differences can be used efficiently in the laboratory. Air can replace Mercury, the effectiveness of maintaining the Temperature changes are much less than Mercury. If Temperatures are maintained, Air can be better and cheap replacement for industrial purposes. The Dufour number (Du) does not enter directly into the momentum and mass equations. Thus the effect of Dufour number on velocity and mass profiles is not apparent. Figure (12) shows the variation of temperature profiles for different values of Du. The parameter Du has marked effects on the temperature profiles. It is observed that the temperature profiles increase with the increasing values of Du. It is also observed from this figure that when Du = 1.0, that is, when the ratio between temperature and concentration gradient is very small the temperature profile shows its usual trend of gradual decay. As Dufour number Du becomes large the profiles overshoot the uniform temperature close to the boundary.

5.3 Concentration distribution

The concentration of the flow field suffers a substantial change with the variation of the flow parameters such as Schmidt number (Sc), Soret number (Sr) and Chemical reaction parameter (k_r). These variations are shown in figures from (13) to (15). From figure (13), shows that an increase in Schmidt number decreases the concentration field. Also Concentration field falls slowly and steadily for Hydrogen and Helium but falls very rapidly for Oxygen and Ammonia in comparison to Water vapour. Thus Water vapour can be used for maintaining normal Concentration field and Hydrogen can be used for maintaining effective Concentration field. The Soret number (Sr) does not enter directly into the momentum and energy equations. Thus the effect of Soret number on velocity and temperature profiles is not apparent. Figure (14) shows the variation of concentration profiles for different values of Sr. The parameter Sr has marked effects on the concentration profiles. It is observed that the concentration profiles increase with the increasing values of Sr. It is also observed from this figure that when Sr = 1.0, that is, when the ratio between concentration and temperature gradient is very small the concentration profile shows its usual trend of gradual decay. As Soret number Sr becomes large the profiles overshoot the uniform concentration close to the boundary. Figure (15) displays the effect of the chemical reaction parameter (k_r) on concentration profiles. As expected, the presence of the chemical reaction significantly affects the concentration profiles. It should be mentioned that the studied case is for a destructive chemical reaction (k_r). In fact, as chemical reaction (k_r) increases, the concentration decreases. It is evident that the increase in the chemical reaction (k_r) significantly alters the concentration boundary layer thickness but does not alter the momentum boundary layers.

5.4 Skin friction and rate of heat and mass transfer

Table – (1) shows the variation of different values Gr, Gc, $\Pr$, Sc, M, K, Sr, Du, and k_r on skin friction (τ). From this table it is concluded that the skin friction (τ) increases as the values of Gr, Gc, K, Sr, Du increase and this behavior is found just reverse with the increase of $\Pr$, Sc, M and k_r.

Table 1. Variation of numerical values of skin friction (τ) for different values of Gr, Gc, Sc, $\Pr$, M, K, Sr, Du and k_r

Gr	Gc	$\Pr$	Sc	M	K	Sr	Du	k_r	τ
1.0	1.0	0.71	0.22	2.0	1.0	1.0	1.0	1.0	1.5879
2.0	1.0	0.71	0.22	2.0	1.0	1.0	1.0	1.0	1.8742
1.0	2.0	0.71	0.22	2.0	1.0	1.0	1.0	1.0	1.9873
1.0	1.0	7.00	0.22	2.0	1.0	1.0	1.0	1.0	1.2590
1.0	1.0	0.71	0.60	2.0	1.0	1.0	1.0	1.0	1.3586
1.0	1.0	0.71	0.22	4.0	1.0	1.0	1.0	1.0	1.1167
1.0	1.0	0.71	0.22	2.0	2.0	1.0	1.0	1.0	1.6540
1.0	1.0	0.71	0.22	2.0	1.0	2.0	1.0	1.0	1.7412
1.0	1.0	0.71	0.22	2.0	1.0	1.0	2.0	1.0	1.6984
1.0	1.0	0.71	0.22	2.0	1.0	1.0	1.0	2.0	1.3695

Table – (2) shows the variation of Nusselt number (Nu) different values $\Pr$ and Du. From this table it is concluded that the Nusselt number (Nu) increases as the value of Du increases and this behavior is found just reverse with the increase of $\Pr$. Table – (3) shows the variation of Sherwood number (Sh) different values Sc, Sr and k_r. From this table it is concluded that Sherwood number (Sh) increase as the value of Sr increase and this behavior is found just reverse with the increase of Sc and k_r.

Table 2. Variation of Nusselt number (Nu) for different values of $\Pr$, Du and λ

$\Pr$	Du	Nu
0.71	1.0	1.2875
7.00	1.0	1.0067
0.71	2.0	1.3481

Table 3. Variation of Sherwood number (Sh) for different values of Sc, Sr, k_r and λ

Sc	Sr	k_r	Sh
0.22	1.0	1.0	1.0598
0.30	1.0	1.0	0.8436
0.22	2.0	1.0	1.2597
0.22	1.0	2.0	0.7694

In order to ascertain the accuracy of the numerical results, the present skin – friction (τ) results are compared with the previous skin – friction (τ^*) results of Chaudhary *et al.* [5] in table – (4). They are found to be in an excellent agreement.

Table 4: Comparison of present Skin – Friction results (τ_1) with the Skin – Friction results (τ_1^*) obtained by Chaudhary *et al.* [5] for different values of Gr, $\Pr$ and M

Gr	$\Pr$	M	τ_1	τ_1^*
1.0	0.71	2.0	1.2254	1.2197
2.0	0.71	2.0	1.3592	1.3465
1.0	0.71	2.0	0.9987	0.9954

VI. Conclusions

In this paper, the governing equations for the effect of chemical reaction on an unsteady magnetohydrodynamic free convection flow of a viscous incompressible fluid past an infinite vertical accelerated plate embedded in porous medium with thermal diffusion, diffusion thermo and constant heat flux in the presence of transverse magnetic field has been presented. Employing the highly efficient finite element method, the leading equations are solved numerically. The results illustrate the flow characteristics for the velocity, temperature, concentration, skin friction, Nusselt number and Sherwood number. The conclusions from these results are:

1. It is observed that the velocity (u) of the fluid increases with the increasing of parameters Gr, Gc, K, Sr, Du and decreases with the increasing of parameters $\Pr, Sc, M$ and k_r.
2. The fluid temperature increases with the increasing of Du and decreases with the increasing of $\Pr$.
3. The concentration of the fluid increases with the increasing of Sr and decreases with the increasing of Sc and λ.
4. From table (1), it is concluded that the skin friction (τ) increases with the increasing values of Gr, Gc, K, Sr, Du and this behavior is found just reverse with the increasing of $\Pr, Sc, M$ and k_r.
5. From table (2), it is concluded that the Nusselt number (Nu) increases with the increasing values of Du and this behavior is found just reverse with the increasing of $\Pr$.
6. From table (3), it is concluded that the Sherwood number (Sh) increases with the increasing values of Sr and this behavior is found just reverse with the increasing of Sc and k_r.
7. On comparing the skin friction (τ) results with the skin friction (τ^*) results of Chaudhary *et al.* [5] it can be seen that they agree very well.

References

[1] M. Acharya, L. P. Singh and G. C. Dash, Heat and mass transfer over an accelerating surface with heat source in presence of suction and blowing, *Int. J. Engng. Sci.*, *37*, 1999, 1 – 18.

[2] K. J. Bathe, Finite Element Procedures, *Prentice – Hall, New Jersey*, 1996.

[3] A. J. Chamkha, H. S. Thakhar and V. M. Soundalgekar, Radiation effects on free convection flow past a semi – infinite vertical plate with mass transfer, *Chemical Engineering Journal*, *84*, 2001, 335 – 342.

[4] P. Chandran, N. C. Sacheti and A. K. Singh, Unsteady hydromagnetic free convection flow with heat flux and accelerated boundary motion, *J. Phys. Soc. Japan*, *67*, 1998, 124 – 129.

[5] R. C. Chaudhary, M. C. Goyal, A. Jain, Free convection effects on MHD flow past an infinite vertical accelerated plate embedded in porous media with constant heat flux, *Matematicas Ensenanza Universitaria*, *XVII (2)*, 2009, 73 – 82.

[6] S. S. Das, and M. Mitra, Unsteady mixed convective MHD flow and mass transfer past an accelerated infinite vertical plate with suction, *Ind. J. Sci. Tech.*, *2 (5)*, 2009, 18 – 22.

[7] S. S. Das, A. Satapathy, J. K. Das and J. P. Panda, Mass transfer effects on MHD flow and heat transfer past a vertical porous plate through a porous medium under oscillatory suction and heat source, *Int. J. Heat Mass Transfer*, *52*, 2009, 5962 – 5969.

[8] S. S. Das, A. Satapathy, J. K. Das and S. K. Sahoo, Numerical solution of unsteady free convective MHD flow past an accelerated vertical plate with suction and heat flux, *J. Ultra Sci. Phys. Sci.*, *19(1)*, 2007, 105 – 112.

[9] S. S. Das, S. K. Sahoo and G. C. Dash, Numerical solution of mass transfer effects on an unsteady flow past an accelerated vertical porous plate with suction, *Bull. Malays. Math. Sci. Soc.*, *29(1)*, 2006, 33 – 42.

[10] J. Gireesh kumar, P. V. Satyanarayana and S. Ramakrishna, Effects of chemical reaction and mass transfer on MHD unsteady free convection flow past an infinite vertical plate with constant suction and heat sink, *J .Ultra Scientist*, *21(3)*, 2009, 12 – 28 .

[11] H. Hasimoto, Boundary layer growth on a flat plate with suction or injection, *J. Phys. Soc. Japan*, *12*, 1957, 68 – 72.

[12] F. S. Ibrahim, A. M. Elaiw and A. A. Bakr, Effect of the chemical reaction and radiation absorption on the unsteady MHD free convection flow past a semi infinite vertical permeable moving plate with heat source and suction, *Communications Nonlinear Science Numerical Simulation*, *13*, 2008, 1056 – 1066.

[13] B. K. Jha, Effects of applied magnetic field on transient free convective flow in a vertical channel, *Ind. J. Pure Appl. Math.*, *29(4)*, 1998, 441 – 445.

[14] Y. J. Kim, Unsteady MHD convective heat transfer past a semi – infinite vertical porous moving plate with variable suction, *Int. J. Engg. Sci.*, *38*, 2008, 833 – 845.

[15] O. D. Makinde, J. M. Mango and D. M. Theuri, Unsteady free convection flow with suction on an accelerating porous plate, *AMSEJ. Mod. Meas. Cont.*, B *72 (3)*, 2003, 39 – 46.

[16] D. Mansutti, G. Pontrelli and K. R. Rajagopal, Steady flows of non-Newtonian fluids past a porous plate with suction or injection, *Int. J. Num. Methods Fluids*, *17*, 1993, 927 – 941.

[17] J. N. Reddy An Introduction to the Finite Element Method, *McGraw – Hill, New York*, 1985.

[18] K. C. Sarangi and C. B. Jose, Unsteady free convective MHD flow and mass transfer past a vertical porous plate with variable temperature, *Bull. Cal. Math. Soc.*, *97 (2)*, 2005, 137 – 146.

[19] P. R. Sharma and D. Pareek, Steady free convection MHD flow past a vertical porous moving surface, *Ind. J. Theo. Phys.*, *50*, 2002, 5 – 13.
[20] A. K. Singh, A. K. Singh and N. P. Singh, Heat and mass transfer in MHD flow of a viscous fluid past a vertical plate under oscillatory suction velocity, *Ind. J. Pure Appl. Math.*, *34(3)*, 2003, 429 – 442.
[21] B. Singh and C. Thakur, An exact solution of plane unsteady MHD non – Newtonian fluid flows, *Ind. J. Pure Appl. Math.*, *33(7)*, 2002, 993 – 1001.
[22] V. M. Soundalgekar, Free convection effects on steady MHD flow past a vertical porous plate, *J. Fluid Mech.*, *66*, 1974, 541 – 551.
[23] K. Yamamoto and N. Iwamura, Flow with convective acceleration through a porous medium, *Engg. Math.*, *10*, 1976, 41 – 54.

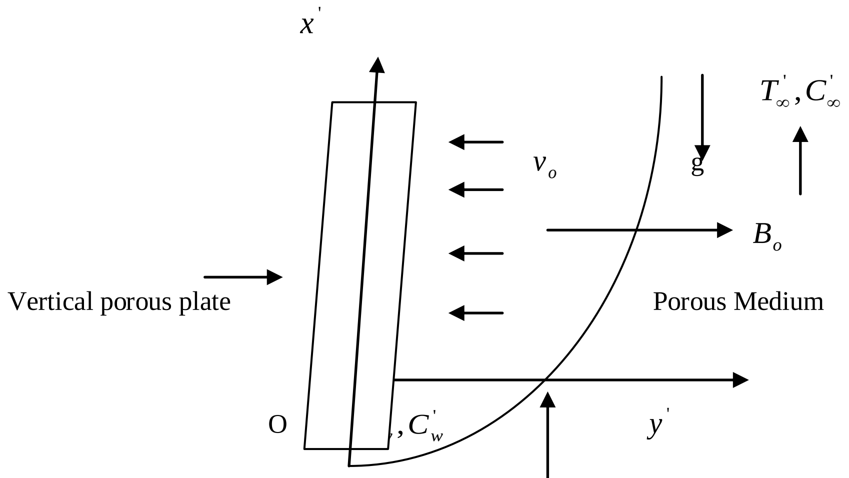

Figure 1. Physical sketch and geometry of the problem

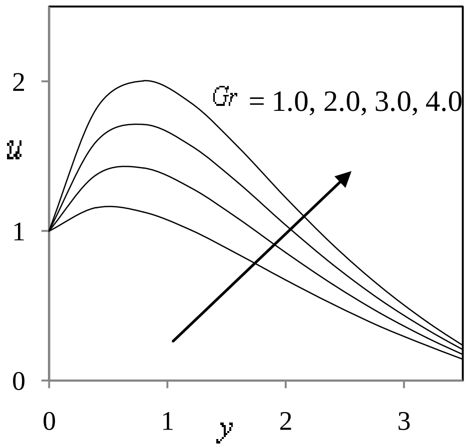

Figure 2. Effect of Grashof number Gr on velocity profiles u

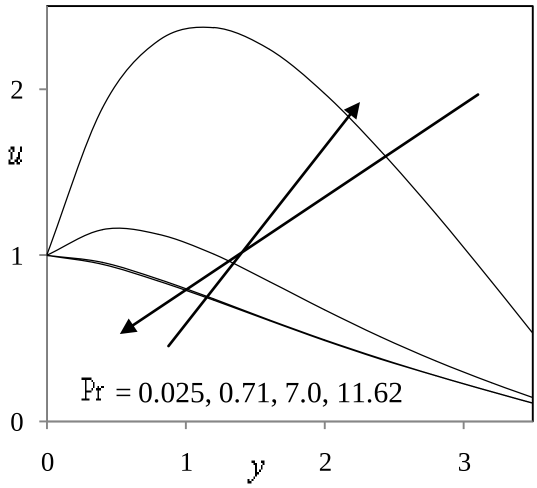

Figure 4. Effect of Prandtl number $\Pr$ on velocity profiles u

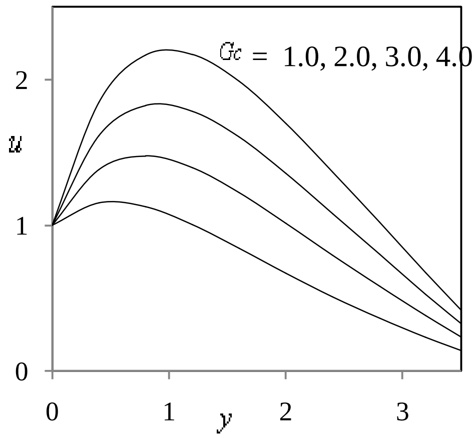

Figure 3. Effect of Modified Grashof number Gc on velocity profiles u

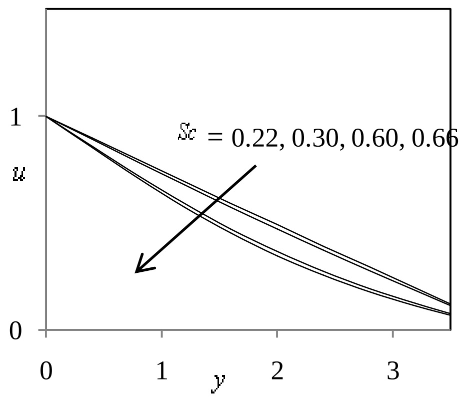

Figure 5. Effect of Schmidt number Sc on velocity profiles u

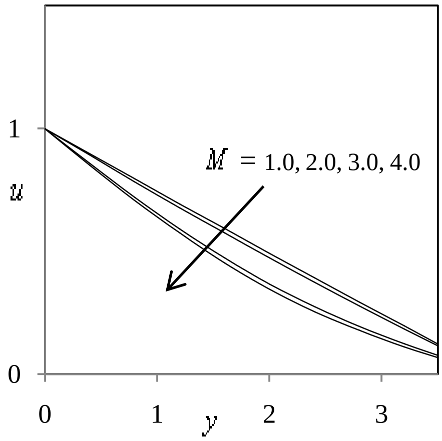

Figure 6. Effect of Hartmann number M on velocity profiles u

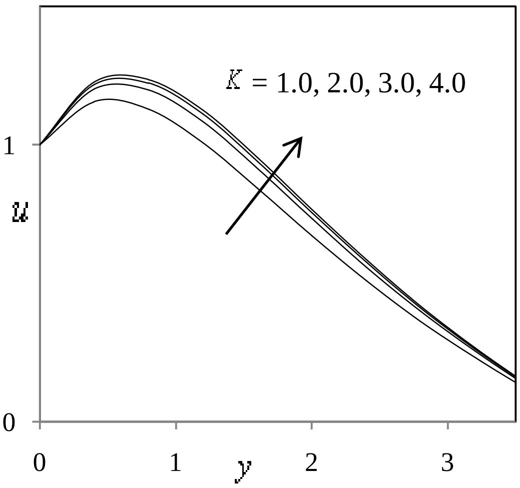

Figure 7. Effect of Permeability parameter K on velocity profiles u

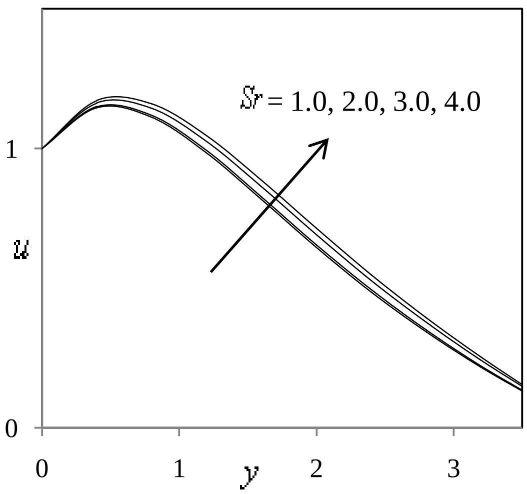

Figure 8. Effect of Soret number Sr on velocity profiles u

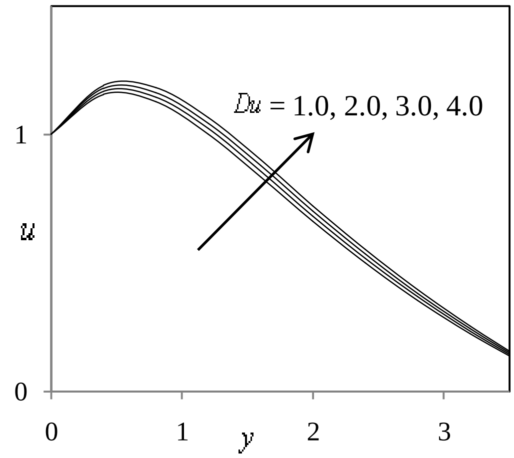

Figure 9. Effect of Dufour number Du on velocity profiles u

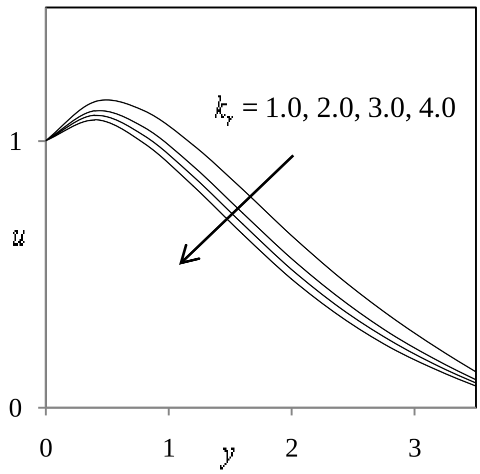

Figure 10. Effect of Chemical reaction parameter k_r on velocity profiles u

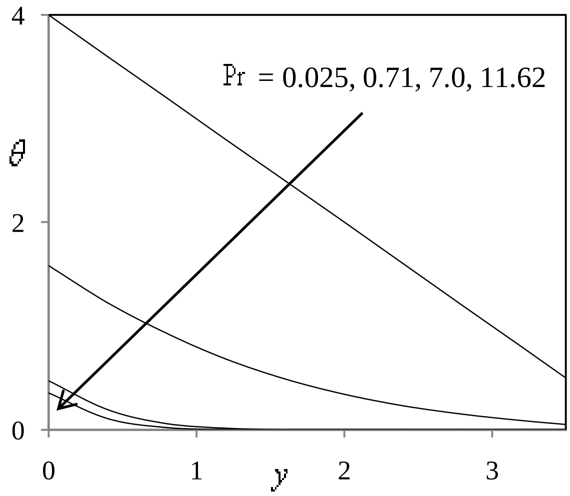

Figure 11. Effect of Prandtl number $\Pr$ on temperature profiles θ

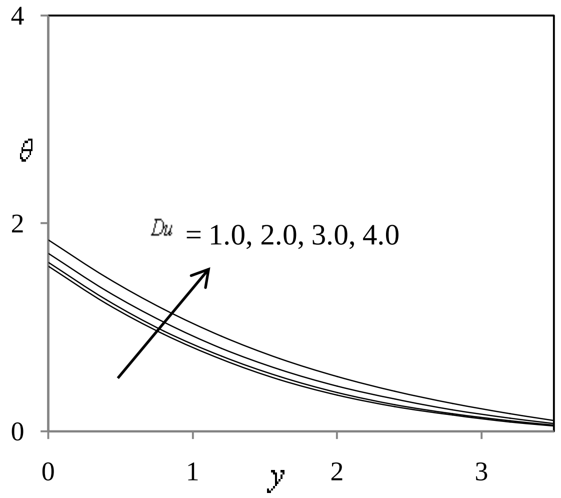

Figure 12. Effect of Dufour number Du on temperature profiles θ

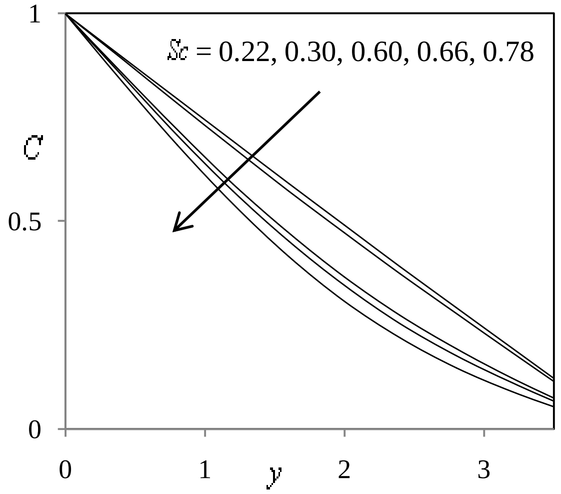

Figure 13. Effect of Schmidt number Sc on concentration profiles C

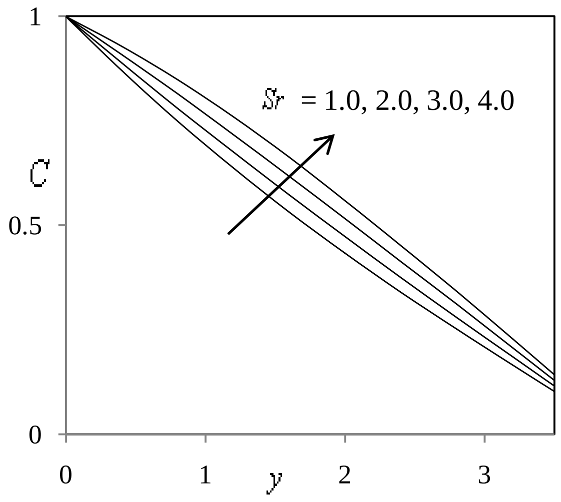

Figure 14. Effect of Soret number Sr on concentration profiles C

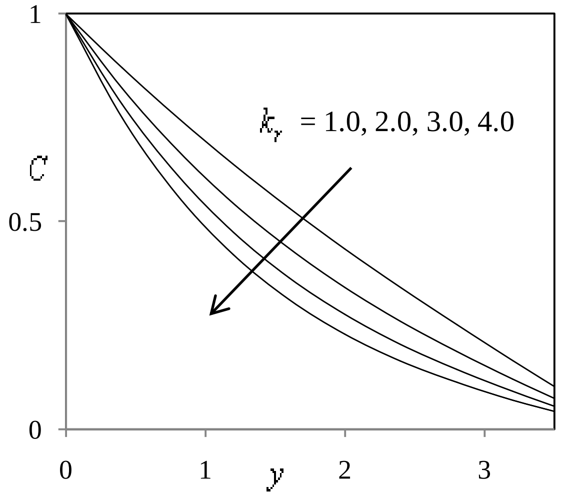

Figure 15. Effect of Chemical reaction parameter k_r on concentration profiles C